SIAM J APPL MATH.
Vol 55, No. 6, pp 1592–1608, December 1995

CRACK PROPAGATION MODELS FOR ROCK FRACTURE IN A GEOTHERMAL ENERGY RESERVOIR*

ALISTAIR D FITT†, AMANDA D KELLY‡, AND COLIN P PLEASE†

Abstract. The propagation of a one-dimensional, fluid-filled crack in a hot dry rock geothermal energy reservoir (HDRGER) is discussed In previous studies a number of different relationships between the normal stress on the crack, the fluid pressure, and the crack height (so-called crack laws) have been used, as have different "flow laws" to determine the relationship between flow rate and crack geometry. Here it is shown that the choice of submodel may have profound implications for the mathematical structure of the problem. In particular, two crack laws (a linear law and a hyperbolic law) are considered as well as two flow laws (a cubic law and a linear law) The model contains a dimensionless parameter that measures the relative importance of stresses due to local deformation of asperities and the long-range deformation of the crack surface The case is considered where the former is the dominant mechanism. A perturbation analysis is performed, and it is found that for some combinations of laws a strained-coordinate analysis is required, whilst for others a matched asymptotic approach is needed. In the latter case the problem may be reduced to that of solving a linear, nonhomogeneous singular integrodifferential equation to determine the behaviour in the boundary layer. This problem is solved, and some conclusions are drawn regarding the relevance of various laws to flow in HDRGERs.

Key words. hydrofracture, geothermal energy, nonlinear diffusion, singular integrodifferential equations

AMS subject classifications. 45, 73T, 76D

1. Introduction.

Hot dry rock geothermal energy reservoirs (HDRGERs) generally consist of huge networks of interconnected cracks in rock where water is pumped into the network from one borehole and extracted at another. In its natural state, the rock contains cracks that allow only a very small flow of water In order to enhance the flow, either water or a viscous gel is pumped at high pressure from an open segment of a borehole into the rock. In this way the reservoir is stimulated Typically, this high-pressure flow leaves the borehole in two opposite directions so that, until the crack is very much longer than the open segment of the borehole in use, a one-dimensional model of a single crack is appropriate The current study describes such a model.

The heat transfer processes that take place within the reservoir are assumed to exert negligible influences on the fluid–rock interaction; this is a reasonable assumption if the short-term motion of the crack is to be considered, since any shrinkage of the rock due to cooling may be assumed to occur over time periods that greatly exceed the fluid residence time

The behaviour of a preexisting, one-dimensional crack in a linearly elastic medium is examined. The crack propagates due to loading by an incompressible, viscous Newtonian fluid. To develop a model for such a process we first consider the separate fluid flow and solid motion problems. To close the model, a crack law is employed to couple the fluid and solid motions

Conventional crack law models assume that the wall elastic normal stress is supported entirely by the wall fluid pressure. Such a crack is referred to as being open

* Received by the editors December 15, 1993; accepted for publication (in revised form) November 28, 1994

† Faculty of Mathematical Studies, University of Southampton, Southampton S017 1BJ, United Kingdom

‡ School of Mathematics, University of Leeds, Leeds LS2 9JT, United Kingdom

(as opposed to partially closed) This is a reasonable assumption for most applications of crack propagation (for example, oil recovery or magma-driven propagation as discussed in Spence and Turcotte [17]). In an HDRGER, however, the fluid pressure seldom becomes large enough to completely separate the crack surfaces This is because the elastic shear stress on the crack walls due to in-situ stresses is sufficient to cause the surfaces to slide over each other well before the crack is open (Pine and Batchelor [13]) This in turn opens up a network of cracks into which the fluid may flow. It is reasonable therefore to assume that the crack surfaces touch and, therefore, that the elastic normal stress is supported by both the fluid pressure and local deformations of asperities in the crack. Modelling the sliding of the crack surfaces over each other is difficult and will not be considered further in the current study.

As the fluid pressure changes, there must be corresponding alterations in both the deformation of the asperities and the elastic normal stress in the rock. The crucial parameter in the current model measures the relative importance of these two effects. The case where the redistribution of normal stresses is the dominant mechanism was discussed by Kelly and Please [7] In the current study, however, we consider the case where the more localised property of elastic deformation of asperities is assumed to be the preferential pressure-balancing term. Evidence suggests that physically, it is this case that is more likely to occur in an HDRGER.

Section 2 of the current study outlines a mathematical model for crack propagation in an HDRGER, giving details of crack and flow law submodels that have been considered before. In § 3 we consider the combination of a Reynolds flow law and a hyperbolic crack law, showing that strained coordinates are required to determine a spatially uniform solution. Section 4 considers the case of a Reynolds flow law and a linear crack law, and we observe that the solution has a nonuniform expansion. The required method of solution for this case is illustrated in § 5 by the qualitatively similar but algebraically easier combination of a linear flow flow and a linear crack law. It transpires that the behaviour in the boundary layer is determined by a linear singular integrodifferential equation, and this is solved both asymptotically and numerically, thereby fully determining the boundary layer behaviour. Finally, § 6 presents some discussion and conclusions

2. A mathematical model for crack propagation in an HDRGER. The basic mathematical model employed to describe the motion of a one-dimensional, fluid-filled, partially open crack that is used in the current study is explained in detail in [7], but for completeness the main assumptions are repeated below Cartesian coordinates are used (see Fig. 1), with the direction x assumed to lie along the length of the crack and y normal to the crack. It is assumed that the crack is thin (its length is large compared to its height) and hence that the variables describing the crack are independent of y. The crack height is denoted by $h(x,t)$, the elastic normal stress along the walls by $\sigma_{yy}(x,t)$, and the pressure of the fluid within the crack by $p(x,t)$ For simplicity we assume that the crack is symmetrical about $x = 0$ and denote its half-length by $\ell(t)$.

It was shown by Spence and Sharp [16] that for a given crack height $h(x,t)$ the elasticity problem arising from the plane strain elastic contact equations (see, for example, [12]) could be solved to yield

$$\sigma_{yy}(x,t) - \sigma_{yy}^{\infty} = \frac{G}{2\pi(1-\nu)} \int_{-\infty}^{\infty} \frac{\partial h(s,t)}{\partial s} \frac{ds}{s-x}, \tag{1}$$

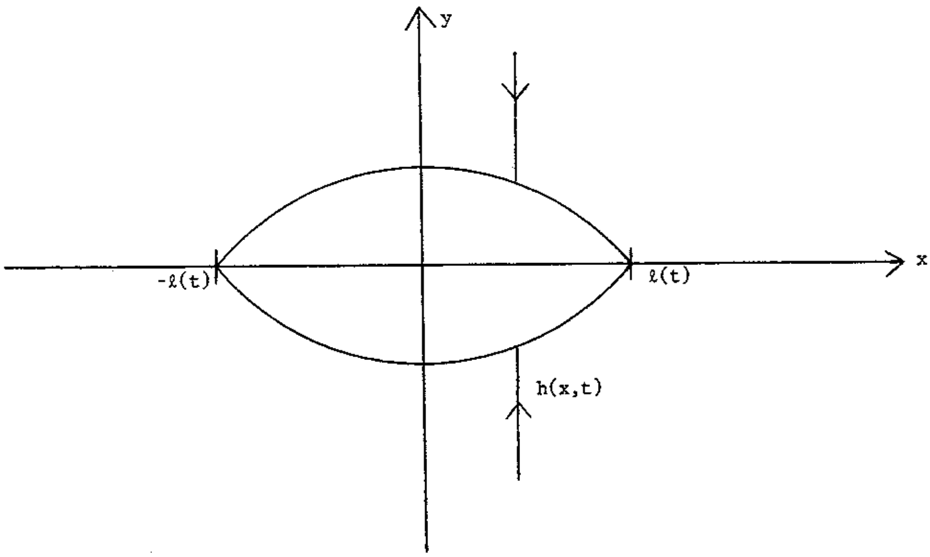

FIG. 1. *Nomenclature and coordinates for the idealised crack.*

where the bar on the integral sign denotes the Cauchy principal value, σ_{yy}^{∞} denotes the normal stress at infinity within the rock, and G and ν are, respectively, the shear modulus and Poisson's ratio of the rock. We refer to (1) as the elasticity equation; physically it describes the normal surface stresses resulting from the deformation of the interface of the elastic material from a planar state. Further development of the model relies upon providing two more equations relating the pressure, crack height, and normal stress. Usually, one of these equations effectively expresses conservation of mass (a flow law), whilst the other relates the normal stress and pressure to the crack height (the crack law). Different flow and crack laws may be used in various combinations, and the purpose of this study is to discuss the effects that different such combinations may have on the mathematical properties of the model.

2.1. Flow law submodels. In this study two different flow models are considered. For the first of these models, it is assumed simply that the fluid flow within the crack is determined by standard lubrication theory. The relationship between the crack height and the fluid pressure is therefore given by Reynolds' equation (see, for example, [10]):

$$h_t = \frac{1}{12\mu}(h^3 p_x)_x, \tag{2}$$

where μ is the dynamic viscosity of the fluid in the crack. We refer to this as the Reynolds flow law. Although this is an appealing flow law to use, it relies on the assumption that the reduced Reynolds' number $\delta_c^2\mathrm{Re}$ is small, where δ_c denotes the aspect ratio of the crack. Typically in an HDRGER the cracks are not smooth but possess many asperities so that the local geometry is complicated. This geometry can change as the crack height varies. Considerable discussion (see, for example, [19]) has therefore taken place regarding the validity of (2) for even mildly tortuous cracks.

Although the Reynolds flow law has been used extensively (see, for example, [16], [17], and many others), its possible limitations have led some authors to consider flow laws that are similar to (2) but where the term h^3 is replaced by a term $a_n h^n$, where the constants n (dimensionless) and a_n (dimensions $length^{(3-n)}$) are to be regarded as experimentally fitted. Note that from (2), we have $a_3 = 1$. Such changes from this cubic law are due to the effects of tortuosity, contact area, and irreducible flow. Evidently the simplest case for analysis is given by the choice $n = 1$, and we refer to this as the linear flow law. A full discussion of flow laws that are derived by empirically fitting to experimental data is given in the review article by Cook [3]. The data suggests that for large crack apertures a flow exponent n greatly in excess of 3 is appropriate, whilst for small apertures the exponent is less than 3. Since the main focus of the current work is the small-aperture crack, we consider both the cases $n = 1$ and $n = 3$ below.

2.2. Crack law submodels. One approach to modelling the stress within the crack has been to assume that that the normal stress at the crack wall is supported entirely by the fluid pressure, so that

$$\sigma_{yy}(x,t) = -p(x,t)$$

(see, for example, [16], [17]). It is known, however, that in many HDRGERs the fluid pressure is insufficient to support the normal elastic stress and the total load is distributed between the fluid pressure and the local deformation of touching asperities. A full review of the models used to fit the mechanical forces acting at an interface for mated joints and partial contact joints may be found in Cook [3]. In such models the local deformation of the asperities is assumed to be a function of the effective stress $\sigma_{yy} + p$. In order to link such crack laws to the flow laws discussed above, it is traditional to define the quantities $h_{\max}$ and $h_{\min}$, which are often referred to in the literature as, respectively, the maximum and minimum crack heights. For $h \geq h_{\max}$ the crack is considered to be fully open with no touching asperities and the standard (zero effective stress) crack law (as used, for example, in [17]) applies. The minimum crack height $h_{\min}$ is nonzero, since even at very large compressive normal stresses there will always be some residual aperture.

Two popular choices of crack law, for cases where the effective stress is nonzero, are known as the linear and hyperbolic crack laws and are discussed below. The linear crack law asserts that the crack height and the effective pressure $\sigma_{yy}(x,t) + p(x,t)$ are related by a piecewise linear law. Pine and Cundall [14] proposed such a law in the specific form

$$h = \begin{cases} h_{\max} - (\sigma_{yy} + p)\frac{(h_{\max} - h_{\min})}{\sigma_R} & (\sigma_R < \sigma_{yy} + p < 0), \\ h_{\min} & (\sigma_{yy} + p \leq \sigma_R), \end{cases} \tag{3}$$

where σ_R, usually termed the reference stress, is the least negative effective stress at which $h = h_{\min}$.

The hyperbolic crack law is generally considered to be a more realistic deformation model for joints in partial contact. It was originally proposed by Goodman [4] and discussed further by Bandis, Lumsden, and Barton [1] and Murphy et al. [11], and assumes that the normal stress, pressure, and crack height are related by

$$\sigma_{yy} + p = \frac{k(h_{\max} - h)}{(h - h_{\min})}. \tag{4}$$

Here the constant k (which has dimensions of stress) is experimentally determined; values of -10^7 Pa for a fracture at a depth of 2 km are typical (Pine and Batchelor [13]).

At the large stresses encountered in the vast majority of HDRGERs, $h_{\max}$ is typically several orders of magnitude greater than $h_{\min}$. We therefore assume from now on that $h_{\min}$ is so small that it may be taken to be zero. The practical consequence of this approximation is that the crack profiles that will be calculated possess compact support. If $h_{\min}$ is taken to be small but nonzero, then the only effect on the solutions is to add an exponentially small contribution that does not possess compact support (see, for example, King and Please [9]).

2.3. Nondimensional version of the models. Below we will consider three combinations of the various laws, showing that in each case there are profound differences in the mathematical structure of the problem. These combinations will be denoted by the nomenclature

RH: Reynolds flow law, hyperbolic crack law;

RL: Reynolds flow law, linear crack law;

LL: linear flow law, linear crack law.

We begin by nondimensionalizing the model for the motion of the crack. Denoting a typical crack length by L and a typical fluid pressure by p_0, we set

$$h = h_{\max}\bar{h}, \qquad x = L\bar{x}, \qquad p = p_0 - (\sigma_{yy}^{\infty} + p_0)\bar{p}, \qquad \sigma_{yy} = \sigma_{yy}^{\infty} + \frac{G h_{\max}}{2\pi L(1-\nu)}\bar{\sigma}_{yy}$$

and determine the relevant timescale according to which combination of laws we are using by writing

$$t = T\bar{t}$$

with

$$T = \frac{-12\mu L^2}{\omega h_{\max}^2},$$

where ω has the values $a_1\sigma_R/h_{\max}^2$ (linear flow law, linear crack law), σ_R (Reynolds flow law, linear crack law), and k (Reynolds flow law, hyperbolic crack law).

In each case, the pressure and normal stress may easily be eliminated to give a single nonlinear singular integrodifferential equation for the crack height $h(x,t)$. Dropping the bars for convenience, we find that for the three cases the relevant equations are

$$\text{(5)} \quad \text{RH:} \quad h_t = \left[h h_x - \epsilon h^3 \frac{\partial}{\partial x}\left(⨍_{-\infty}^{\infty} \frac{\partial h}{\partial s}\frac{ds}{s-x} \right)\right]_x, \quad \text{where} \quad \epsilon = \frac{-G h_{\max}}{2\pi k(1-\nu)L},$$

$$\text{(6)} \quad \text{RL:} \quad h_t = \left[h^3 h_x - \epsilon h^3 \frac{\partial}{\partial x}\left(⨍_{-\infty}^{\infty} \frac{\partial h}{\partial s}\frac{ds}{s-x} \right)\right]_x, \quad \text{where} \quad \epsilon = \frac{-G h_{\max}}{2\pi \sigma_R(1-\nu)L},$$

$$\text{(7)} \quad \text{LL:} \quad h_t = \left[h h_x - \epsilon h \frac{\partial}{\partial x}\left(⨍_{-\infty}^{\infty} \frac{\partial h}{\partial s}\frac{ds}{s-x} \right)\right]_x, \quad \text{where} \quad \epsilon = \frac{-G h_{\max}}{2\pi \sigma_R(1-\nu)L}.$$

In each case, the equation applies when $0 < h < 1$. Regions in which h is identically zero may occur, whilst in regions where h is greater than unity, the equations and analysis of, for example, [16] are appropriate. Henceforth we shall only consider cases in which h remains less than one.

Evidently for each of these models the order of magnitude of ϵ is a key factor in determining the behaviour of solutions. In each case, ϵ is a ratio of shear modulus/crack length to reference stress/maximum crack displacement, and its value determines how changes in the fluid pressure are compensated for. Large values of ϵ imply that changes in the fluid pressure are balanced by a global redistribution of stresses along the crack, whilst small values of ϵ imply that such pressure changes are accommodated by a local deformation of asperities. In typical HDRGERs there are circumstances when ϵ is large, and this limiting case has been discussed in [7]. More commonly (for example, for cracks of length 1 m at a depth of 2 km) ϵ is small (typically of the order 1/10 or 1/100), and it is the small-ϵ case which we shall consider below. It will transpire that the solutions to these various cases have different structures. In particular, in the asymptotic limit of small ϵ some cases will possess regular expansions, whilst others will require more careful analysis to determine a spatially uniformly valid first order solution.

It should be noted that, for arbitrary values of ϵ these equations possess similarity solutions corresponding to particular boundary and initial data. Rather than numerically determining these somewhat restrictive solutions, we prefer to exploit the small parameter ϵ in the problem in order to determine the key properties of the solution structure.

2.4. Initial and boundary conditions. The modelling formulation is completed by the specification of the necessary initial and boundary conditions. Physically, the problem to be examined concerns the large-time spreading of a fixed mass of fluid injected initially into a short section of a crack. We anticipate that, as in many other diffusion-type processes, the large-time behaviour will not be sensitive to the precise nature of the initial data. At these large times, this initial data manifests itself via a matching condition; we will assume that this matching is equivalent to imposing a point-source, Barenblatt-type [2] condition upon the problem. For this reason, we will not disallow initial data that violates $h < 1$. In any case, we anticipate that the asymptotic expansions will prove to be nonuniform as $t \to 0$. Later in the text, some further comments will be made concerning the relationship between the solution and the initial data.

We insist that the crack retains compact support so that $h(x,t) > 0$ for $x < \ell(t)$, and zero otherwise. Under the assumption that no mass enters the crack from infinity, the initial condition therefore reflects the fact that the mass of fluid in the crack remains constant and initially the crack length tends to zero.

By symmetry we have $h_x(0,t) = 0$, and we must also ensure that mass is conserved at the moving boundary. The final condition comes from consideration of the stress singularity at the crack tip. Owing to the precracked nature of HDRGERs, we assume that this singularity has zero strength.

Taking the total dimensionless mass of fluid within the crack to be unity, the boundary conditions are

$$(8) \quad h(x,t) = \begin{cases} 0 & (\ell(t) \leq |x|), \\ > 0 & (-\ell(t) < x < \ell(t)), \end{cases} \qquad h_x(0,t) = 0, \qquad \int_{-\ell(t)}^{\ell(t)} h(x,t)dx = 1,$$

and

$$h(x,t) = o((\ell(t) - x)^{1/2}) \quad \text{as } x \to \ell(t).$$

The initial condition is $\ell(t) \to 0$ as $t \to 0$.

By making obvious changes to the initial and boundary conditions given above, a range of other, related problems (for example, a constant flux or a constant pressure given at $x = 0$) may also be analysed. In these cases, however, it is awkward to determine even the $O(1)$ solutions, and since the solution structure near to the crack tips is not significantly altered we do not consider these further.

3. Reynolds flow law with a hyperbolic crack law. First, we consider the case RH. The relevant integral equation is (5) with boundary and initial conditions (8). We begin by seeking a regular perturbation solution for small ϵ, writing

$$h = h_0 + \epsilon h_1 + \cdots, \qquad \ell = \ell_0 + \epsilon \ell_1 + \cdots \qquad (\epsilon \to 0)$$

The leading-order partial differential equation is

$$h_{0t} = (h_0 h_{0x})_x,$$

and the solution is given for $0 \leq \eta < 1$ by

$$h_0 = \frac{\lambda^2}{6t^{1/3}}(1-\eta^2), \qquad \ell_0(t) = \lambda t^{1/3}, \tag{9}$$

where

$$\lambda = \left(\frac{9}{2}\right)^{1/3}, \qquad \eta = \frac{x}{\lambda t^{1/3}}. \tag{10}$$

In order to demonstrate that a regular expansion will be appropriate for this problem, consider how the various terms on the right hand side of (5) compete with each other. When h is $O(1)$, the term multiplied by the small parameter is clearly the smaller of the two. Near the crack tips, however, where it may be anticipated that any nonuniformities will manifest themselves, the asymptotic behaviour of the terms is

$$h_0 h_{0x} \sim 1 - \eta, \qquad h_0^3 \frac{\partial}{\partial x}\left(\fint_{-\infty}^{\infty} \frac{\partial h_0}{\partial s} \frac{ds}{s-x} \right) \sim (1-\eta)^2$$

The second of these two terms is thus uniformly smaller than the first, and the stress intensity boundary condition will automatically be satisfied at next order. This reflects the fact that, throughout the whole crack, the dominant physical balance in the equation remains the same. We conclude that a regular expansion with coordinate straining will suffice.

The $O(\epsilon)$ problem is given by

$$h_{1t} = \left[(h_0 h_1)_x - h_0^3 \left(\fint_{-\ell(t)}^{\ell(t)} \frac{\partial h_0(s,t)}{\partial s} \frac{ds}{s-x} \right)_x \right]_x,$$

and using $h_1(x,t) = t^{-4/3} H(\eta)$, we find that H satisfies the ordinary differential equation

$$(1-\eta^2)H'' - 2\eta H' + 6H = \frac{\lambda^5}{54}(\eta^2 - 1)\left[6\eta^2 - 2 + 3\eta(\eta^2-1)\log\left(\frac{1-\eta}{1+\eta}\right) \right] \tag{11}$$

The general solution to this equation is given by

$$\begin{aligned} H(\eta) = {} & A(3\eta^2 - 1) + B\left(\frac{1}{4}(3\eta^2-1)\log\left(\frac{1+\eta}{1-\eta}\right) - \frac{3\eta}{2} \right) + \frac{\lambda^5}{3240}\eta^2(49 - 15\eta^2) \\ & + \frac{\lambda^5}{6480}\left[(8 - 24\eta^2)\log(1-\eta^2) + (70\eta^3 - 15\eta - 15\eta^5)\log\left(\frac{1-\eta}{1+\eta}\right) \right], \end{aligned} \tag{12}$$

where A and B are arbitrary constants, and to satisfy $H_\eta = 0$ at $\eta = 0$ we take $B = 0$. It remains to ensure that (12) satisfies $h = 0$ at $x = \ell(t)$ and conserves mass; however, expanding

$$\ell(t) = \lambda t^{1/3} + f(\epsilon)\ell_1(t),$$

it may quickly be shown that there is no choice of $f(\epsilon)$ which allows the $O(\epsilon)$ part of h to be zero at $x = \ell(t)$.

A standard regular perturbation expansion having failed, we attempt to suppress the singularities at the ends of the range by using strained coordinates. Evidently we have a choice whether to strain the coordinate x or t, but it may be shown that if x is strained, then the additional term that appears in (12) is odd and must therefore be discarded. To strain coordinates in t we write

$$t = T - \epsilon g(T)$$

and observe that the leading-order problem is unchanged and so has solution

$$h_0(x,T) = \frac{\lambda}{6T^{1/3}}(1-\eta^2), \qquad \eta = \frac{x}{\lambda T^{1/3}}.$$

The $O(\epsilon)$ problem is therefore

$$g_T h_{0T} + h_{1T} = (h_0 h_1)_{xx} + \left[\frac{h_0^3}{3T}\left(x \log\left(\frac{\lambda T^{1/3} - x}{\lambda T^{1/3} + x}\right)\right)_x\right]_x,$$

and with $h_1(x,T) = T^{-4/3}H(\eta)$ we find that a similarity solution is successful, provided that g' is proportional to $1/T$. Using $g(T) = k \log T$ we find that H satisfies (11) but with an additional term

$$k\lambda^2\left(\eta^2 - \frac{\lambda}{3}\right)$$

added to the right-hand side The general solution is therefore given by the sum of (12) and an extra term

$$-\frac{k\lambda^2}{30}(4\eta^2 + (3\eta^2 - 1)\log(1-\eta^2)).$$

By choosing

$$\ell(T) = \lambda T^{1/3} + \epsilon\mu T^{-2/3}, \qquad k = \frac{\lambda^3}{18},$$

and

$$A = \frac{\lambda}{648}(4\lambda^4 \log 2 - \lambda^4 + 108\mu),$$

the secularities are therefore suppressed. We note also that with this choice of A and k, it is true for any μ that

$$\int_{-\ell_0-\epsilon\ell_1}^{\ell_0+\epsilon\ell_1} h_0 + \epsilon h_1 \, dx = 1 + O(\epsilon^2).$$

A spatially uniformly valid solution, correct to $O(\epsilon)$, is therefore given for $|x| \leq \ell(t)$ by

$$h = \frac{\lambda^2}{6T^{1/3}}(1-\eta^2) + \frac{\epsilon}{T^{4/3}}\left[\frac{\lambda\mu}{6}(3\eta^2-1) + \frac{\lambda^5}{648}(-3\eta^4+2\eta^2+1+(12\eta^2-4)\log 2) + \frac{\lambda^5}{1296}[(3\eta^2+9\eta+4)(1-\eta)^3\log(1-\eta) + (3\eta^2-9\eta+4)(1+\eta)^3\log(1+\eta)]\right],$$

where

$$t = T - \frac{\epsilon\lambda^3}{18}\log T.$$

It will be noted that this solution contains the parameter μ, which is undetermined to this level of approximation. μ may be thought of as a matching constant, and is determined by the behaviour of the solution for small values of t, when the full equation applies. Such dependency on the earlier history of the solution is often encountered in reaction-diffusion problems (see, for example, King [8]). We note that, as anticipated, the expansion is nonuniform as $T \to 0$.

Typical results are shown in Fig 2, where the values $\mu = 3$ and $\epsilon = 1/100$ were used. The crack profile is shown for times $t = 1$, 2, 5, 10, and 20. These results will be compared with those for other models in § 6.

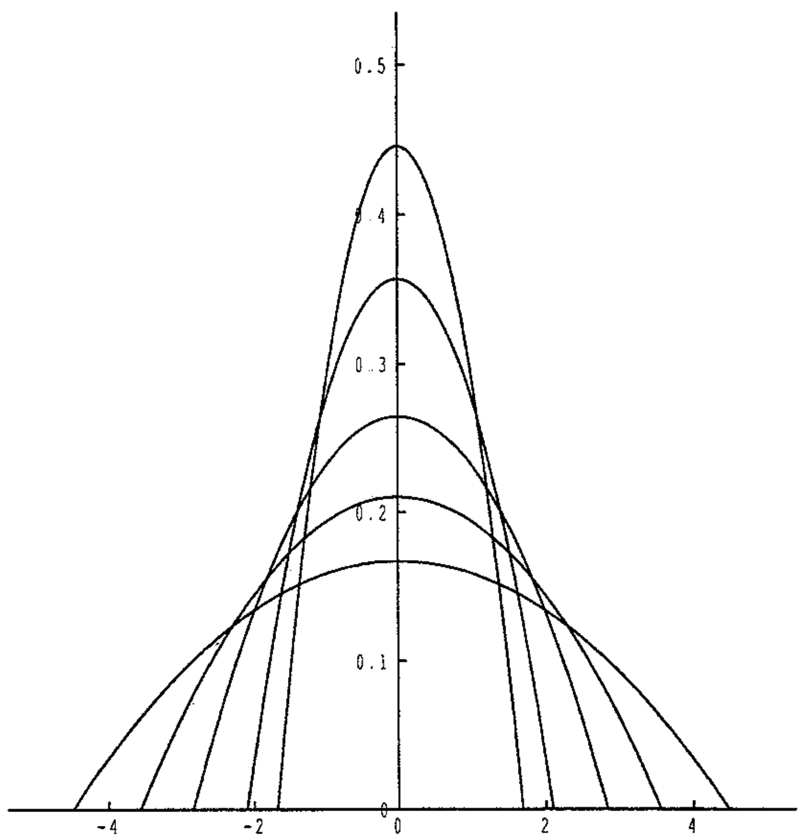

FIG 2 *Crack profiles for the case RH with data* $\mu = 3$, $\epsilon = 1/100$ *at times* $t = 1, 2, 5, 10, 20$

4. Reynolds flow law with a linear crack law. Next we consider the case RL. We solve the equation (6) subject to the conditions (8), using a regular perturbation expansion of the form $h = h_0 + \epsilon h_1 + \cdots$, $\ell = \ell_0 + \epsilon \ell_1 + \cdots$ $(\epsilon \to 0)$. This gives the leading-order solution

$$h_0 = t^{-1/5}\left(\frac{3\lambda^2}{10}\right)^{1/3}(1-\eta^2)^{1/3}, \qquad \ell_0(t) = \lambda t^{1/5},$$

$$\text{where} \quad \eta = \frac{x}{\lambda t^{1/5}}, \qquad \lambda = \left(\frac{5}{48}\right)^{1/5}\left(\frac{1}{\beta(\frac{4}{3},\frac{4}{3})}\right)^{3/5}$$

At next order we find that, with $h_1(x,t) = t^{-4/5}H(\eta)$, H satisfies

$$(1-\eta^2)H'' - \frac{10}{3}\eta H' + \frac{2}{3}H = 2\lambda\eta v(\eta) - \lambda(1-\eta^2)v'(\eta),$$

$$\text{where} \quad v(\eta) = \left(\frac{4}{45}\right)^{1/3}\left[\fint_{-1}^{1} \frac{u(1-u^2)^{-2/3}}{u-\eta}du\right]_\eta.$$

The solution of this equation may be expressed as a quadrature involving v and hypergeometric functions.

As in the previous section, we now consider whether the expansion is spatially uniform. Near the crack tip, the two terms on the right-hand side of (6) are given asymptotically by

$$h_0^3 h_{0x} \sim (1-\eta)^{1/3}, \qquad h_0^3\frac{\partial}{\partial x}\left(\fint_{-\infty}^{\infty}\frac{\partial h_0}{\partial s}\frac{ds}{s-x}\right) \sim (1-\eta)^{-2/3}$$

Evidently the second term is now no longer uniformly smaller in space than the first This indicates that there is a change in the dominant physical balance in the equation along the crack. Close to the crack tip the dominant balance must include the term involving the singular integral in order that all the boundary conditions may be satisfied. Thus a singular perturbation analysis is appropriate.

The analyses for the cases RL and LL follow similar paths. The algebra involved in the case RL is complicated, however, by the presence of the hypergeometric functions For simplicity therefore, the general method will therefore be illustrated in the discussion of the case LL below

5. Linear flow law with a linear crack law. Consider the case LL where (7) is to be solved with boundary and initial conditions (8). Seeking a regular perturbation expansion as in § 3, we find that h_0 is given by (9) and (10).

This case is closely related to the case RL, since near to the crack tip we have

$$h_0 h_{0x} \sim 1-\eta, \qquad h_0\frac{\partial}{\partial x}\left(\fint_{-\infty}^{\infty}\frac{\partial h_0}{\partial s}\frac{ds}{s-x}\right) \sim 1$$

As discussed in the previous section, a singular perturbation analysis is thus appropriate.

To determine the behaviour over the whole region, we employ matched asymptotic expansions We first determine the outer (i.e., away from the crack tips) solution. With $h_1(x,t) = t^{-2/3}H(\eta)$, the $O(\epsilon)$ equation reduces to the ordinary differential equation

$$(1-\eta^2)H'' - 2\eta H' + 2H = \frac{4\lambda}{3} - \frac{2\lambda\eta}{3}\log\left(\frac{1+\eta}{1-\eta}\right),$$

which has the general solution

$$H(\eta) = A\left(2+\eta\log\left(\frac{1-\eta}{1+\eta}\right)\right) - \frac{4\lambda\eta}{9}\log\left(\frac{1-\eta}{1+\eta}\right) + \frac{2\lambda}{9}\log(1-\eta^2)$$

$$- \frac{\lambda\eta}{9}\log\left(\frac{1-\eta}{1+\eta}\right)\log(1-\eta^2)$$

$$- \frac{4\lambda\eta}{9}\left[-\frac{1}{2}\log(1-\eta)\log(1-\eta^2) + \operatorname{dilog}\left(\frac{1+\eta}{2}\right)\right.$$

$$- \log 2\log(1-\eta) + \frac{1}{2}\log(1-\eta)\log(1+\eta) + \frac{1}{4}[\log(1-\eta)]^2$$

$$\left. + \frac{1}{2}\log(1+\eta)\log(1-\eta^2) - \frac{1}{4}[\log(1+\eta)]^2 - \frac{\pi^2}{12} + \frac{1}{2}(\log 2)^2\right], \tag{13}$$

where A is an arbitrary constant and the other component of the complementary function has been discarded since it is odd. As usual, the dilogarithm function is defined by

$$\operatorname{dilog}(x) = \int_1^x \frac{\log s}{1-s}\,ds.$$

As before, we note that the expansion is not uniform as $t \to 0$, but we do not analyse this region.

The solution (13) is not valid near the crack tips; specifically it is of order $\log\epsilon$ when $\eta \sim 1-\epsilon$ We therefore seek an inner expansion in the crack tip region by writing

$$h_{\text{inner}} = h_0 + \epsilon\bar{h}_1.$$

This ansatz is somewhat nonstandard but is introduced so that the function $\bar{h}_1$ remains bounded when matching with the outer region This leads to a simpler integral equation than the more obvious choice of taking, for example, $h_{\text{inner}} = \epsilon\hat{h}_1$

Without loss of generality we examine the behaviour of the solution near the crack tip, $\eta = 1$. In this inner region (see Fig. 3 for a schematic diagram) we make the change of independent variables

$$x = \ell - \epsilon X, \qquad t = T$$

Although h_0 is zero for $x \geq \lambda t^{1/3}$, we anticipate that $\bar{h}_1$ will not decrease to zero until $x = \ell(t)$; without loss of generality we assume that $\ell(t) > \lambda t^{1/3}$ and write $\ell(t) = \lambda t^{1/3} + \epsilon\ell_1(t)$ $(\ell_1 > 0)$. Retaining terms only of order one, we find after some simplification that

$$\frac{\lambda^2}{9T^{4/3}}\mathcal{H}(X-\ell_1(T)) + \frac{\lambda}{3T^{2/3}}\bar{h}_{1X}$$

$$= \left[\left(-\bar{h}_1 + \frac{\lambda}{3T^{2/3}}[-X+\ell_1(T)]\mathcal{H}(X-\ell_1(T))\right)\right.$$

$$\cdot\left(-\frac{\lambda}{3T^{2/3}}\mathcal{H}(X-\ell_1(T)) - \bar{h}_{1X} + \frac{\lambda}{3T^{2/3}(\ell_1(T)-X)}\right.$$

$$\left.\left. + \left(\int_0^{2\ell/\epsilon}\frac{\partial\bar{h}_1(S,T)}{\partial S}\frac{dS}{S-X}\right)_X\right)\right]_X,$$

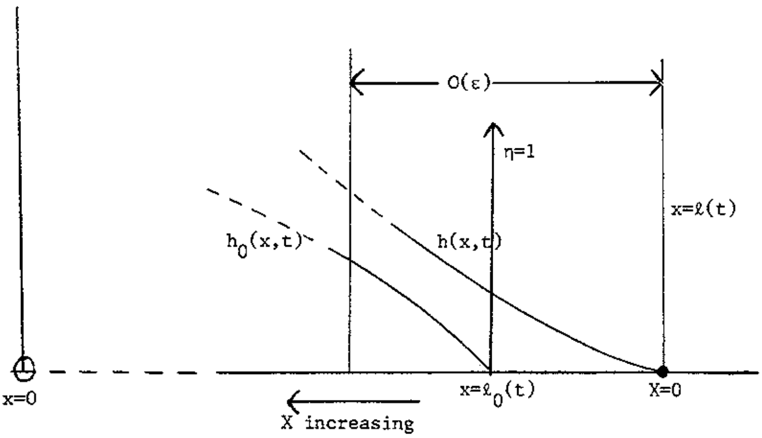

FIG 3 *Schematic of boundary layer regions and variables for the case LL*

where $\mathcal{H}$ denotes the Heaviside unit step function. Setting

$$\bar{h}_1 = \frac{\phi(X,T)}{T^{2/3}}$$

and integrating, we find that

$$\frac{\lambda^2}{9}(X-\ell_1(T))\mathcal{H}(X-\ell_1(T)) + \alpha(T) + \frac{\lambda\phi}{3} = \left(-\phi + \frac{\lambda}{3}(-X+\ell_1(T))\mathcal{H}(X-\ell_1(T))\right)$$
$$\left(-\frac{\lambda}{3}\mathcal{H}(X-\ell_1(T)) - \phi_X + \frac{\lambda}{3(\ell_1(T)-X)} + \left(\int_0^{2\ell/\epsilon} \frac{\partial\phi(S,T)}{\partial S}\frac{dS}{S-X}\right)_X\right),$$

where $\alpha(T)$ is arbitrary. Choosing $\alpha(T)=0$ so that mass conservation is satisfied, we find that the equation for ϕ requires that either

$$-\frac{\lambda}{3} = -\frac{\lambda}{3}\mathcal{H}(X-\ell_1(T)) - \phi_X + \frac{\lambda}{3(\ell_1(T)-X)} + \left(\int_0^{2\ell/\epsilon} \frac{\partial\phi(S,T)}{\partial S}\frac{dS}{S-X}\right)_X$$

or

$$\phi + \frac{\lambda}{3}(X-\ell_1(T))\mathcal{H}(X-\ell_1(T)) = 0$$

The second of these conditions will not be considered further. since it merely asserts that h is identically zero outside the crack From these equations we note that T only enters the problem as a parameter We may also integrate once again to obtain

$$-\frac{\lambda X}{3} = -\frac{\lambda}{3}(X-\ell_1)\mathcal{H}(X-\ell_1) - \phi$$
$$-\frac{\lambda}{3}\log|\,\ell_1 - X\,| + K + \int_0^{2\ell/\epsilon} \frac{\partial\phi(S)}{\partial S}\frac{dS}{S-X}. \quad (14)$$

where K denotes the constant of integration and is determined from the matching condition.

We start by imposing the conservation of mass condition on the solution. We observe that the boundary layer is of width $O(\epsilon)$ and the solution in this region is of height $O(\epsilon)$, so that the total mass in the boundary layer is $O(\epsilon^2)$. Hence the constant A in (13) may be determined to this order solely from the outer solution. This gives

$$A = -\frac{\lambda}{9} - \frac{2\lambda}{9}\log 2.$$

Matching may now be carried out in the normal way. The two-term inner limit of the two-term outer solution is given by

$$\lambda\left[-\frac{2}{9} + \frac{\pi^2}{27} + \frac{1}{3}\log\left(\frac{2\lambda T^{1/3}}{\epsilon X}\right)\right] + O(\epsilon\log\epsilon),$$

and this determines the behaviour of ϕ for large X. We also note that an analysis of the contributions to the integral term in (14) from each of the regions of the crack confirms that the upper limit in the integral term of (14) may be replaced by infinity.

The behaviour within the boundary layer near the crack tip is therefore determined by the problem

$$(15)\quad -\frac{\lambda X}{3} = -\frac{\lambda(X-\ell_1)}{3}H(X-\ell_1) - \phi - \frac{\lambda}{3}\log|\ell_1 - X| + K + \int_0^\infty \frac{\partial\phi(S)}{\partial S}\frac{dS}{S-X}$$

with

$$\phi(0) = 0, \qquad \phi \sim \lambda\left[-\frac{2}{9} + \frac{\pi^2}{27} + \frac{1}{3}\log\left(\frac{2\lambda T^{1/3}}{\epsilon X}\right)\right] \quad (X \to \infty)$$

The matching condition in this case may be interpreted as providing a relationship between K and ℓ_1 for a given T and ϵ. Using the known behaviour of $\phi(X)$ for large values of X, it is evident that the integral term in (15) becomes negligible for large X. Thus

$$(16)\qquad K = \frac{\pi^2\lambda}{27} + \frac{\lambda}{3}\log\left(\frac{2\lambda T^{1/3}}{\epsilon}\right) - \frac{\lambda\ell_1}{3} - \frac{2\lambda}{9}.$$

For practical purposes it simplest to rewrite (15) in terms of the dependent variable $\theta(X)$ defined by

$$\theta(X) = K - \frac{\lambda}{3}\log(1+X) + \frac{\lambda X}{3} - \frac{\lambda}{3}(X-\ell_1)\mathcal{H}(X-\ell_1) - \phi(X).$$

This gives the linear singular integrodifferential equation

$$(17)\qquad 0 = \theta + \frac{\lambda}{3}\log\left(\frac{1+X}{X}\right) + \frac{\lambda}{3(1+X)}\log X - \int_0^\infty \frac{\theta'(S)dS}{S-X}$$

with

$$\theta(0) = K, \qquad \theta \to 0 \text{ as } X \to \infty.$$

In principle, a closed-form solution to (17) may be determined. Writing the equation as

$$\theta - \int_0^\infty \frac{\theta'(S)dS}{S-X} = f(X)$$

and taking the Laplace transform, we find that the Laplace transform of $\theta(X)$ satisfies a linear nonhomogeneous singular integral equation with coefficients that are linear in the transform variable p. The procedure for solving such equations is well established, and details may be found in Varley and Walker [18]. The homogeneous problem with condition $\theta(0) = \alpha$ may be shown to possess the unique solution

$$\theta(X) = \int_0^\infty q(s) e^{-Xs/\pi} ds,$$

where

$$q(s) = \frac{\alpha}{\pi(1+s^2)^{3/4}} \exp\left(-\frac{1}{\pi}\int_0^s \frac{\log t}{1+t^2} dt\right),$$

and it thus remains only to determine a suitable particular integral. Unfortunately this is greatly complicated by the fact that the Laplace transform of $f(X)$ is a combination of exponential integral and Meijer G-functions. In consequence, although a formula for the particular integral may be written down, it is of little practical use. Since there is no difficulty in establishing the relevant properties of θ and there are simple and reliable numerical methods available for (17), we do not pursue the closed-form solution of the equation further.

In order to completely determine the behaviour in the boundary layer we have to determine K; rearranging (16) then gives ℓ_1 as

$$\ell_1 = -\frac{3K}{\lambda} + \frac{\pi^2}{9} - \frac{2}{3} + \log\left(\frac{2\lambda T^{1/3}}{\epsilon}\right)$$

To determine K we observe that although (17) possesses a unique solution for any K, there will be precisely one K for which the solution possesses the correct stress singularity strength. A local analysis may be performed to show that this solution actually has zero slope, the local behaviour being $\theta'(X) \propto \sqrt{X}$.

For numerical purposes it is convenient to transform (17) to a finite range. Setting

$$X = \frac{1+x}{1-x}, \qquad \theta(X) = \gamma(x)$$

gives

$$\gamma(x) - \int_{-1}^{1} \frac{(1-x)(1-s)\gamma'(s)ds}{2(s-x)} = -\frac{\lambda}{6}(1-x)\log\left(\frac{1+x}{1-x}\right) - \frac{\lambda}{3}\log\left(\frac{2}{1+x}\right) \tag{18}$$

with

$$\gamma(x) \sim -\left(\frac{3K-\lambda}{6}\right)(1-x) - \frac{\lambda}{6}(1-x)\log\left(\frac{1+x}{1-x}\right) \qquad (x \to 1)$$

The solution is computed for various values of K (see Appendix I for details of the simple numerical method that was used) until the value of K is determined so that $\gamma'(-1) = 0$. With ϵ and T given ℓ_1 may then be calculated. With 200 collocation points K was calculated to be -0.2400 so that, for example, with values of $\epsilon = 1/10$ and $T = 2$ we find that $\ell_1 = 4.597$. Fig. 4 shows inner, outer, and composite expansions for the crack profile for x positive with these values of ϵ and t.

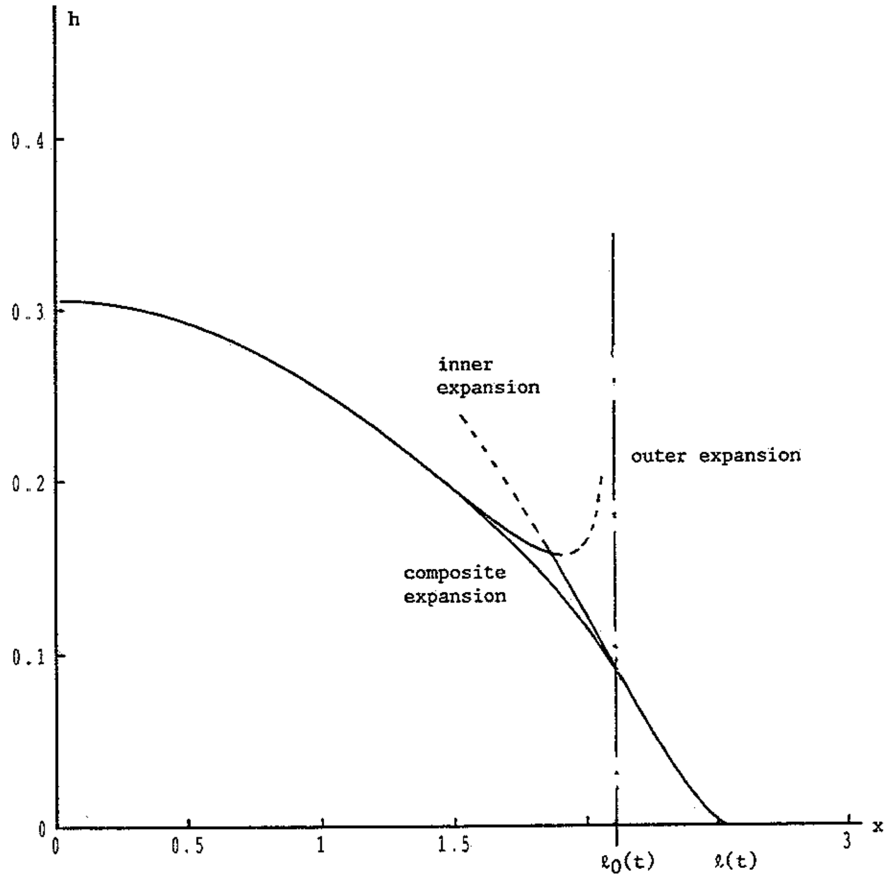

FIG 4 *Inner, outer, and composite expansions for crack profile for the case* $\epsilon = 1/10$, $t = 2$

6. Discussion and conclusions. Having completed the mathematical analysis of the above combinations of crack and flow laws, it is instructive to examine the practical consequences for HDRGER modelling In the case RH, once the crack profile has been determined the fluid pressure p may also be calculated Inevitably in this case the pressure becomes negative and infinite like $(x \pm \ell(t))^{-1}$ near the crack tips. This is no surprise, for the hyperbolic crack law can only give rise to a closed crack if the pressure does become infinite. A more interesting result of the analysis is that the expansion in this case is regular in space, and hence the large negative pressures that are predicted are not restricted to a small area in the vicinity of the crack tip. Physically, this suggests that the model must, at some point, break down as the fluid will not be able to sustain such pressures Modifications could include allowing for the existence of a region containing a vacuum and/or accounting for the fact that (as discussed above) $h_{\min}$ is small but nonzero

The cases LL and RL both predict pressures that are zero (relative to the reference stress) at the crack tips. The pressure in the crack varies smoothly, with only an $O(1)$ variation. As the crack tip is approached, the pressure tends to zero with a finite gradient The matched asymptotic analysis shows, however, that in a narrow region near the crack tip, the pressure gradient changes rapidly until it becomes zero at the tip itself Such behaviour suggests that no special changes to the modelling are required in such a region

The existence of large negative pressure at the crack tips may have other important consequences In particular, since the cracks are preexisting and contain fluid (albeit a small amount), such pressures will cause the fluid to be drawn towards the spreading crack from regions ahead of the crack tip Although coherent experimental evidence is largely lacking, the fluid pressure in the crack ahead of the crack tip has been observed in some cases to decrease from its initial in-situ value. Various explanations have been proposed for this; in particular, sliding along part of the crack is thought under some circumstances to lead to a redistribution of far-field stresses The very large negative pressures predicted above provide a possible additional mechanism for the observed behaviour To determine which of these two mechanisms is the more important, however, a much more complicated, fully coupled problem would have to be considered, and this remains an open question

Appendix I. Numerical solution of the singular integrodifferential equation arising in the case LL. The boundary layer analysis for the case LL requires that numerical solutions are calculated for the equation (18) with $\gamma(-1) = K$ and $\gamma(1) = 0$ A number of numerical methods have been discussed for solutions of equations of this type (see, for example, [5]), but many such schemes require that (18) is first recast as a singular integral, rather than integrodifferential, equation This is usually accomplished by inverting and integrating Here we prefer to employ a simple direct method The interval $[-1, 1]$ is discretized using N equally spaced points $x_1 = -1, x_2, \ldots, x_{N-1}, x_N = 1$, and collocation is used to determine the values of γ at the internal mesh points in $[-1, 1]$. Piecewise linear approximations are used for γ away from the collocation point, whilst on either side of the collocation point (where piecewise linear approximations would lead to a nonexistent integral) quadratic approximations are employed. This allows all the singular integrals to be computed exactly The resulting scheme may be written as

$$\gamma(x_k) - I(x_k) = F(x_k) \qquad (k = 2, 3, \ldots, N-1),$$

where

$$F(x_k) = -\frac{\lambda}{6}(1 - x_k)\log\left(\frac{1+x_k}{1-x_k}\right) - \frac{\lambda}{3}\log\left(\frac{2}{1+x_k}\right),$$

$$\begin{aligned} I(x_k) = {} & \sum_{j=1}^{k-2} \frac{(1-x_k)(\gamma_{j+1}-\gamma_j)}{2h}\left[-h + (x_k - 1)\log\left(\frac{|x_k - x_j|}{|x_k - x_{j+1}|}\right)\right] \\ & + \sum_{j=k+1}^{N-1} \frac{(1-x_k)(\gamma_{j+1}-\gamma_j)}{2h}\left[-h + (x_k - 1)\log\left(\frac{|x_k - x_j|}{|x_k - x_{j+1}|}\right)\right] \\ & + \left(\frac{1-x_k}{2}\right)\left[\frac{4\gamma_k(x_k-1)}{h} + \gamma_{k+1}\left(-1 + \frac{2}{h}(1-x_k)\right) \right. \\ & \left. + \gamma_{k-1}\left(1 + \frac{2}{h}(1-x_k)\right)\right]. \end{aligned} \tag{19}$$

Here $h = x_{j+1} - x_j$, and in (19), the first summation is to be taken to be zero when $k = 2$, and the second to be zero when $k = N - 1$. The scheme described above is simple to code, and the resulting linear equations may be solved using a standard library routine. (In this instance the NAG routine F04ATF was used, and coding was carried out in FORTRAN running on a SUN SPARCstation.) Space does not permit any more than the briefest of analyses of the properties of the method (fuller details may be found in [15] and [6], for example), but the design of the scheme ensures that the matrix of coefficients of the relevant linear equations is strictly diagonally dominated (specifically, the modulus of the diagonal element of each row exceeds the sum of the absolute values of the off-diagonal elements by precisely unity) Test cases may easily be constructed by suitably altering the function $F(x_k)$, and additionally the known asymptotic behaviour at each end may be used to check the results; in all cases the scheme performs well. A number of checks were also performed to confirm that the scheme is insensitive to the number of points used In all cases sufficiently accurate results were computed using 200 collocation points

REFERENCES

[1] S BANDIS, A. C LUMSDEN AND N. R. BARTON, *Fundamentals of rock joint deformation*, Internat. J Rock Mech Min Sci Geomech Abstr , 20 (1983), pp 249–268.

[2] G I BARENBLATT, *On a class of exact solutions for the plane one-dimensional problem of unsteady filtration into a porous medium*, Prikl. Mat. Mekh., 17 (1953), pp 739–742

[3] N G W COOK, *Natural joints in rock; mechanical, hydraulic and seismic behaviour and properties under normal stress*, Internat J Rock Mech Min Sci Geomech Abstr , 29 (1992), pp. 198–223.

[4] R E GOODMAN, *The mechanical properties of joints*, Proc. 3rd Congr ISRM, Denver, 1A (1947), pp. 127–140

[5] V V. IVANOV, *The Theory of Approximate Methods and Their Application to the Numerical Solution of Singular Integral Equations*, Noordhoff International, Groningen, the Netherlands, 1977

[6] P JUNGHANNS AND B SILBERMANN, *Zur theorie der Näherungsverfahren für singuläre Integralgleichungen auf Intervallen*, Math Nachr , 103 (1981), pp 199–244

[7] A D KELLY AND C. P PLEASE, *Hydrofracture of partially open cracks in geothermal energy reservoirs*, SIAM J. Appl Math., submitted.

[8] J R. KING, *Extremely high concentration dopant diffusion in silicon*, IMA J Appl. Math., 40 (1988), pp 163–181

[9] J R KING AND C. P. PLEASE, *Diffusion of dopant in crystalline silicon: An asymptotic analysis*, IMA J Appl Math., 37 (1986), pp 185–197

[10] W E. LANGLOIS, *Slow Viscous Flow*, Macmillan, New York, 1964.

[11] H MURPHY, Z DASH, G ZYVOLOSKI, A. WHITE, AND M WING, *Fluid flow in deformable rock joints: Part* I, Memorandum ESS-4-85-84, Los Alamos National Lab., Los Alamos, NM, 1985.

[12] N I. MUSKHELISHVILI, *Some Basic Problems in the Mathematical Theory of Elasticity*, P Noordhoff, Groningen, Leyden, the Netherlands, 1953.

[13] R J. PINE AND A. S. BATCHELOR, *Downward migration of shearing in jointed rock during hydraulic injections*, Internat. J Rock Mech. Min., 25 (1984), pp 249–263.

[14] R. J. PINE AND P. A CUNDALL, *Applications of the fluid-rock interaction programme (FRIP) to the modelling of hot dry rock geothermal energy systems*, Proc Int S. Fundamentals, September 1985, pp. 293–302

[15] G SCHMIDT, *Spline collocation for singular integro-differential equations over* (0, 1), Numer Math., 50 (1987), pp 337–352

[16] D A. SPENCE AND P SHARP, *Self-similar solutions for elastohydrodynamic cavity flow*, Proc Roy. Soc. London Ser. A, 400 (1985), pp 289–313

[17] D A. SPENCE AND D. L. TURCOTTE, *Magma driven propagation of cracks*, J Geo. R-S E B1, 90 (1985), pp 575–580.

[18] E VARLEY AND J D. A WALKER, *A method for solving singular integrodifferential equations*, IMA J. Appl. Math., 43 (1989), pp. 11–45.

[19] P A WITHERSPOON, J S Y WANG, K IWAI, AND J E. GALE, *Validity of the cubic law for fluid flow in a deformable rock structure*, Water Resources Research, 16 (1980), pp 1016–1024.